Send Orders for Reprints to reprints@benthamscience.ae

Current Medical Imaging Reviews, **2015,** *11,* **15-22**

Integration of a Fuzzy Spatial Constraint into Active Shape Models for ROI Detection in Medical Images

Walid Barhoumi[1,*], Nawres Khlifa[2] and Mouna Abidi[1]

[1]*Research Team on Intelligent Systems in Imaging and Artificial Vision (SIIVA)–RIADI Laboratory, University of Manouba, Tunisia;* [2]*Laboratory of Medical Technology, University of Tunis El Manar, Tunisia*

Walid Barhoumi

Abstract: Segmentation of noisy and low-contrast images remains one of the most challenging and difficult tasks, especially in the context of medical imaging. In this work, we propose an extension of the Active Shape Models (ASM) which is based on a priori knowledge about the shape and the deformation modes of the studied Region(s) of Interest (ROI). The main contribution of the proposed extension resides in the integration of a statistical directional relationship within the ASM, which is learned during a training phase. In particular, in order to force the active contour to move towards points in space that satisfy the spatial relationship, we propose a fuzzy directional constraint that allows a more robust localization of ROI. In fact, the learned a priori knowledge has been modeled using fuzzy logic in order to model uncertainty and ambiguity of the spatial representation. Realized tests on scintigraphic and MRI images proved the performance of the proposed model for the detection of multiple objects of interest in noisy and low-contrast images, even when real contours are ill-defined.

Keywords: Active shape models, a priori knowledge, fuzzy logic, medical image segmentation, spatial relationships.

1. INTRODUCTION

Image segmentation is an essential low-level step for many applications in the field of image processing and computer vision. In medical imaging, the segmentation aims to extract one or many regions of interest (ROI) in the image. It can assist clinicians to diagnose the diseases more easily and more accurately. Indeed, the result of the segmentation often determines which treatments are more likely to be proposed in downstream. The existing methods, for the segmentation of medical images, can be grouped into two main classes: supervised methods and unsupervised ones. Unsupervised methods do not use any prior knowledge and are fully based on low-level features which are implicitly driven from pixels' intensities. These methods have the major disadvantage of being not robust enough and often require post-processing to refine the delineation of ROI. Indeed, unsupervised methods are highly sensitive to noise and produce satisfactory results only if the contrast between structures of interest is sufficiently marked. To overcome these drawbacks, supervised methods incorporating prior knowledge, such as shape, position and orientation, are increasingly used. Supervised methods have the ability of segmenting even images with no well defined relation between regions and pixels' intensities. These methods can be grouped into three basic classes: atlas-based methods [1], deformable models [2] and methods based on spatial relationships [3].

Atlas-based methods are generic, but their use is limited seen their high computation cost. This is mainly due to the necessity of a registration step. A deformable model consists to initialize a contour that will be subsequently deformed and moved to coincide with the edges of ROI, according to an energy term. Segmentation methods based on deformable models are broadly classified, according to their representation, as parametric, geometric and statistical active contours. A parametric deformable model is based on minimizing the deformation energy (*e.g.* snakes [4]). However, this model is not adapted to the topology changes. Geometric active contours are based on the theory of curve evolution (*e.g.* level sets [5]). This is done by moving the initial contour to the object of interest in the normal direction. Thanks to their ability to adapt the topology changing, geometric deformable models allow the simultaneous detection of multiple objects. However, they fail to treat images with discontinuous contours. Finally, statistical deformable models (*e.g.* active shape models and active appearance models) [6] differ from the other deformable models because of using a training phase. In particular, Active Shape Models (ASM) incorporate a priori knowledge about the shape in order to delineate accurately ROI. Many works [7, 8] demonstrated the effectiveness of ASM for various medical applications. In fact, this model has the advantage of taking into account the anatomical variability of the topologies and automatically handles the topological change. However, it requires a large training set and the manual intervention of experts. Besides, results are not satisfactory in the case of noisy, low-contrast and/or low-resolution images. The last class of supervised segmentation methods is the one based on spatial relationships. These relationships are used to select the corresponding regions according to a predefined description or to constrain the deformable model [9]. To profit of a priori knowledge based on the spatial relationships in the segmentation process, a knowledge-gathering phase is required. It consists to decompose the image into a set of entities linked by spatial relations. Then, a model-based representation of these relationships is defined. However, the segmentation results are highly dependent on the modeling step.

*Address correspondence to this author at the Department of Computer Science, National Engineering School of Carthage, University of Carthage, 45 Rue des Entrepreneurs, 2035, Tunis, Tunisia; Tel: +216-71-940699; Fax: +216-71-941579; E-mail: walid.barhoumi@esti.rnu.tn

1875-6603/15 $58.00+.00

In this work, we are particularly interested in the integration of spatial knowledge into active shape models, in order to minimize the dependence of the segmentation results on the initialization step and on the image quality (noise, low resolution, low contrast…). Indeed, few works have opted for the combination of statistical models with those based on spatial representation [10-14]. Nevertheless, given the complementarity between these two models, it seems obvious that spatial relationships could be combined with ASM while improving the accuracy of segmentation results, notably for low-quality images. Existing works have introduced different extensions to ASM by integrating learned models on the distance variation between studied structures, in order to control the shape models progress. However, distance-based models are not invariant under scaling. Besides, most of spatial relationships suffer from inaccuracy. In our case, a priori angle-based knowledge is learned before being modeled using fuzzy membership functions in order to model the uncertainty and the ambiguity of the spatial representation. In fact, since spatial relationships usually suffer from ambiguity, we adopted a fuzzy model to constrain the deformation of contours while taking into account the uncertainties and inaccuracies associated with these relationships. This representation allows forcing the active shape heading to the actual contour, even in the presence of heavy noise. Indeed, the added spatial constraint reduces variations of the initial contour and likely shift to other regions whose shapes or intensities are similar to those of the regions of interest. This is ensured thanks to the definition of an eligible area for the positions of these regions. Moreover, during the phase of ROI delineation, the suggested model allows either the confirmation of the new position of the deformable contour, or the displacement of this contour according to the allowable space of angles' variations. More precisely, the proposed method considers two essential informations during the deformation of ASM: a shape constraint related to the target object and a direction constraint. This spatial constraint avoids collisions and remoteness of ROI contours during the deformation process. Thus, the evolution of the proposed estimations is controlled, at each iteration of the localization phase, using the direction constraint. This permits to attract the initial contour towards the ROI while avoiding the fact that the contour is conducted towards other regions of the same visual appearance. The suggested method permits to delineate automatically multiple ROIs in a medical image. This delineation can assist clinicians in many steps of various clinical routines steps, such as tumor segmentation, tumor recognition, lesions malignancy tracking and quantization of diagnosis attribute.

The rest of this paper is structured as follows. In section 2, we introduce the proposed segmentation method which integrates a fuzzy spatial constraint on direction in active shape models. In section 3, some experiments with an objective assessment, on synthetic images as well as on real-world scintigraphic and MRI images, are produced. Lastly, conclusions and ideas for further works are summarized in section 4.

2. PROPOSED METHOD

The objective of this paper is to integrate a spatial constraint into active shape models. The constraint consists in describing the orientation of the ROI according to a reference point (the origin of the image). This can overcome some limitations of ASM, specially its dependence on the initialization step and on the image quality. Thus, the ROI localization can be more accurate, even in noisy images, images of low resolution and low-contrast images. In fact, in addition to the integration of spatial information into ASM, the originality of the proposed method resides in modeling the spatial constraint by the fuzzy logic in order to restrain the contour deformation towards the ROI. This permits to attract the initial contour towards the object of interest, while avoiding above all that the contour moves towards another object of the same visual appearance. Indeed, proposed method is composed of two main phases. The first one is an offline training phase allowing the building of the shape and the orientation models. Given the learned shape and orientation constraints during the training phase, the second phase consists to localize the ROI in a new test image. In what follows, we briefly recall the principle of ASM before presenting the proposed extension.

2.1. Background: Conventional Active Shape Models

ASM [6] consists in deforming iteratively an initial contour in order to be close to the real contour of the ROI. To do this, an offline training phase is firstly applied in order to construct the Point Distribution Model (PDM), which permits the modeling of a priori knowledge on the eligible shapes. The PDM construction consists to manually label a contour on the ROI for each image *i* of the training set (of size *M*), that will be marked with *n* landmarks (*n* is a constant). This is done using a training set of images representing the possible variations of the object to be detected. Thus, each shape *i* is represented by a vector X_i of dimension *2n* as follows (1):

$$\forall i \in \{1,\cdots,M\},\ X_i = (x_i^1, x_i^2, \cdots, x_i^n, y_i^1, y_i^2, \cdots, y_i^n)^T, \quad (1)$$

where, x_i and y_i ($1 \le i \le n$) are the coordinates of the points forming the manually labeled contour. Then, an iterative algorithm aligns the *M* shapes in order to define the mean shape $\overline{X}$. Finally, a statistical analysis based on Principal Components Analysis (PCA) defines the eigenvectors of the covariance matrix. This aims to determine the principal directions and their main modes of variations. Then, a shape model is defined to describe the shape variations (2), which may be represented as a function of the mean shape and the variation of the principal directions (the eigenvectors of the covariance matrix). The defined model illustrates a compact representation of allowable space of the shape variations.

$$\forall j,\ X_j = \overline{X} + P.b_j = \frac{1}{M}\sum_{i=1}^{M} X_i + P.\left(b_j^1,\ldots,b_j^t\right)^T, \quad (2)$$

where, *P* is the matrix of the *t* more significant eigenvectors, $b_j=(b_j^1,\ldots, b_j^t)^T$ is the weight vector that represents the projection of the shape X_j on *P*. The allowable values for the weight b_j^k ($1 \le k \le t$) typically vary between $-3\sqrt{\lambda_k}$ and $+3\sqrt{\lambda_k}$ (λ_k is the k^{th} eigenvalue of the covariance matrix), which is often referred to as the allowable shape space. Then, the localization phase serves to search a shape in a new image using the PDM. It consists to start by an initial estimation of the mean shape $\overline{X}$ (initial contour). This esti-

mate is subsequently deformed towards the borders of the studied ROI. In fact, the shape is subsequently deformed iteratively towards the edges of the ROI, given the allowable space defined in the training phase, and the gray level of pixels belonging to the normal on each point of the contour. The best position of each landmark is then determined by the research of the best profile according to that calculated at the same position in the mean shape. The comparison of the two profiles is carried out using the Mahalanobis distance (3).

$$d(g,\bar{g}) = (g-\bar{g})^T S^{-1}(g-\bar{g}), \quad (3)$$

where, g is the profile constructed at each landmark, $\bar{g}$ is the profile associated with the mean shape of the same landmark and S is the covariance matrix according to the profiles of reference landmarks. The most similar pattern to the profile of the mean shape is the one minimizing this distance. Thus, each landmark is moved to the point of the profile that is most similar to the profile of the mean shape according to the Mahalanobis distance [15].

2.2. Integration of a Spatial Constraint into ASM

In the proposed method, we consider two important constraints during contour deformation: the ROI shape (as defined in the conventional ASM) and its orientation. In fact, at each iteration of the localization phase, we verify the shape and the orientation constraints before moving the contour C. Indeed, our experiments proved that using the shape model alone; to describe the shape variations; do not guarantee an accurate delineation of the ROI. In most of cases, this model is not specific enough to permit arbitrary variation different from that seen in the training dataset. Thus, we integrate an orientation model in order to model a priori knowledge on the eligible orientations of ROI. More precisely, we estimate the angle between the ROI and a reference object. Then, we deform the contour according to the allowable space of orientation variation, which is defined in the training phase. In fact, the integration of the orientation is performed through a modeling phase followed by a localization phase. In the first phase, for each image of the training set, we mark the center of gravity P of the ROI, given the manually labeled landmarks. Then, we compute the angle between the vertical line $\bar{j}$ and the vector $\overrightarrow{PO}$ (Fig. **1**). This permits to define a model describing the authorized space variation of the orientation α, according to the set of estimated angles relatively to the images composing the training dataset. In fact, given the angles α_{min}, α_{max} and $\bar{\alpha}$ representing respectively the minimum, maximum and mean angles defined in the training phase, the authorized space of orientation variations is defined by the interval $[\alpha_{min}, \alpha_{max}]$ illustrating the plausible variations of the ROI orientation. Note that we opted for using angles, instead of distances [7], to illustrate direction constraints in order to be invariant against scaling change.

The defined direction constraint allows controlling the evolution during the localization stage, in order to avoid collisions and the remoteness of objects contours. However, spatial relationships generally have problems of ambiguity [16] what justifies the adoption of fuzzy logic since this formalism takes into consideration uncertainties and inaccuracies linked to these relations [7]. Indeed, we have adopted a

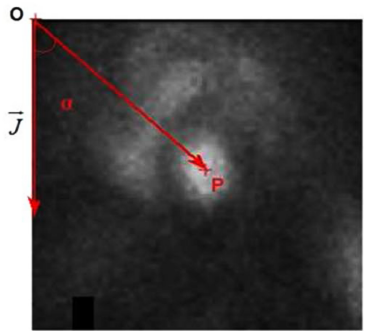

Fig. (1). Illustration of the angle concept for a single object.

fuzzy model in order to represent contours' deformations and to avoid that the deformable model is attracted by the contours of other objects than that composing the ROI. In particular, we aim to maintain angles during the localization phase. This is done using a fuzzy set representing the satisfaction degree of the object orientation with respect to a reference object at any point in space. To do this, we specified each spatial relationship by a piecewise affine function. In fact, given the angle between the vertical line $\bar{j}$ and the vector $\overrightarrow{PO}$ of the current contour C, we defined three fuzzy membership functions describing the spatial disposition of the contour C according to the allowable space of orientation variations $[\alpha_{min}, \alpha_{max}]$. This consists to define three fuzzy degrees of positioning of the contour C, relatively to the allowable space $[\alpha_{min}, \alpha_{max}]$, "on the left" μ_L (4), "on the right" μ_R (5) and "at an angle approximately equals to $\bar{\alpha}$" $\mu_{\sim}$ (6), such that $\forall\, \alpha,\ \mu_L(\alpha)+\mu_R(\alpha)+\mu_{\sim}(\alpha)=1$. Fig. (**2**) illustrates an example of the defined spatial membership functions for the case of $\alpha_{min}=30°$, $\alpha_{max}=80°$ and $\bar{\alpha}=60°$ ($\alpha_1=45°$ and $\alpha_2=70°$).

$$\mu_L(\alpha) = \begin{cases} 1 & if \quad \alpha \le \alpha_{min} \\ \dfrac{\alpha_1 - \alpha}{\alpha_1 - \alpha_{min}} & if \quad \alpha_{min} < \alpha < \alpha_1 \\ 0 & if \quad \alpha \ge \alpha_1 \end{cases} \quad (4)$$

With, $\alpha_1=((\bar{\alpha}-\alpha_{min})/2)+\alpha_{min}$ and $\alpha_2=((\alpha_{max}-\bar{\alpha})/2)+\bar{\alpha}$.

$$\mu_R(\alpha) = \begin{cases} 1 & if \quad \alpha \ge \alpha_{max} \\ \dfrac{\alpha - \alpha_2}{\alpha_{max} - \alpha_2} & if \quad \alpha_2 < \alpha < \alpha_{max} \\ 0 & if \quad \alpha \le \alpha_2 \end{cases} \quad (5)$$

$$\mu_{\sim}(\alpha) = \begin{cases} 0 & if \quad \alpha \le \alpha_{min} \text{ OR } \alpha \ge \alpha_{max} \\ \dfrac{\alpha_{min} - \alpha}{\alpha_{min} - \alpha_1} & if \quad \alpha_{min} < \alpha \le \alpha_1 \\ \dfrac{\alpha_{max} - \alpha}{\alpha_{max} - \alpha_2} & if \quad \alpha_2 < \alpha < \alpha_{max} \\ 1 & if \quad \alpha_1 \le \alpha \le \alpha_2 \end{cases} \quad (6)$$

Thus, in the localization phase, we take into account the two informations of shape and orientation, in order to detect the ROI in a new image. Indeed, after defining the initial contour using the average shape $\bar{X}$ of the shape model, we proceed to the iterative shifting and deformation of the con-

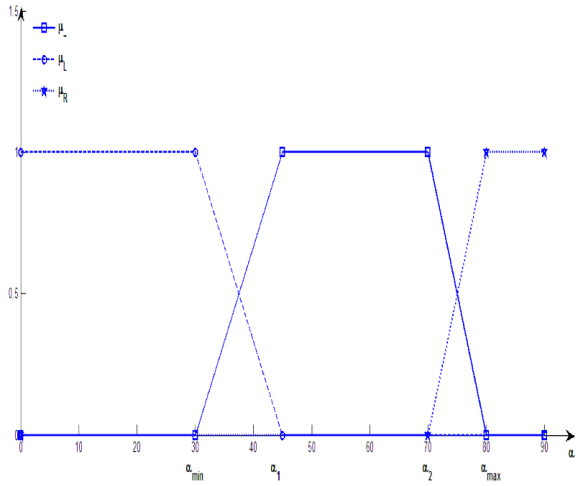

Fig. (2). The fuzzy degrees of positioning of a contour C, relatively to the allowable space $[\alpha_{min}, \alpha_{max}]$, "on the left" μ_L, "on the right" μ_R and "at an angle approximately equals to $\overline{\alpha}$" $\mu_{\sim}$.

tour C while respecting the shape model. Then, we applied the orientation model either to confirm the new position of the contour, or to move C according to the allowable space of angle variations. In fact, after estimating the relative angle α of the current contour C, we deform the contour according to the admissible space of orientations, already defined in the training phase. Thus, the initial contour evolves according to the shape model and to the angle model. Indeed, at each iteration, if the angle α between the vertical axis and the vector $\overrightarrow{OP}$ belongs to the interval $[\alpha_1, \alpha_2]$ (the green space in Fig. (**3**)), the shape model is validated without needing to change the position of the contour according to the angle model. This corresponds to the case where $\mu_L=0$, $\mu_R=0$ and $\mu_{\sim}=1$. Else, if the angle α is lower than α_{min} (*resp.* higher than α_{max}) then the current contour is totally on the left (*resp.* on the right) of the allowable angle space. This corresponds to the case where $\mu_L=1$, $\mu_R=0$ and $\mu_{\sim}=0$ (*resp.* $\mu_L=0$, $\mu_R=1$ and $\mu_{\sim}=0$). In this case, the contour C should be moved towards the allowable angle space by translating it by a distance of $||\overrightarrow{OP}||.sin(\alpha)$ (*resp.* $W-||\overrightarrow{OP}||.sin(\alpha)$), where W denotes the width of the input image) in the direction of right (*resp.* of left). Otherwise, if the angle α belongs to the interval $]\alpha_{min}, \alpha_1[$ (resp. $]\alpha_2, \alpha_{max}[$) then the current contour is partially on the left (*resp.* on the right) of the allowable angle space (the orange space in Fig. (**3**)). This corresponds to the case where $\mu_L \in]0,1[$, $\mu_R=0$ and $\mu_{\sim} \in]0,1[$ (*resp.* $\mu_L=0$, $\mu_R \in]0,1[$ and $\mu_{\sim} \in]0,1[$). In this case, the contour C should be partially moved towards the allowable angle space according to the non-zero values among μ_L, μ_R and $\mu_{\sim}$. This amounts to move the contour by a distance of $\mu_{\sim}(\alpha).(||\overrightarrow{OP}||.sin(\alpha))$ (*resp.* $W-\mu_{\sim}(\alpha).(||\overrightarrow{OP}||.sin(\alpha))$) in the direction of right (*resp.* of left). In all cases, the initial contour is moved iteratively towards the ROI and then the contour evolution is oriented directly to the desired object according to the allowable orientation space $[\alpha_{min}, \alpha_{max}]$ previously defined. Thus, the direction constraint forces the shape model to move in an acceptable space of authorized orientations (Fig. (**4**)). The iterative localization process does not stop until the convergence condition is satisfied or a predefined number of iterations is reached. In our case, the iterative deformation process of the contours stops only when a small proportion of landmarks continues to move.

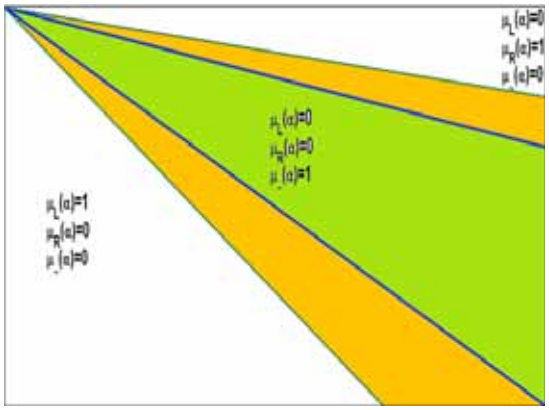

Fig. (3). Illustration of the allowable space of angle variations for the case of $\alpha_{min}=30°$, $\alpha_{max}=80°$ and $\overline{\alpha}=60°$ ($\alpha_1=45°$ and $\alpha_2=70°$).

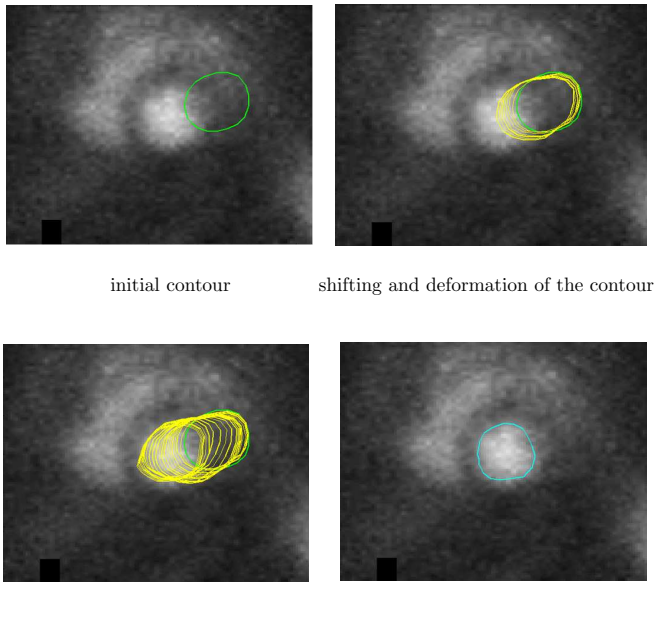

Fig. (4). ROI localization steps on a real scintigraphic image.

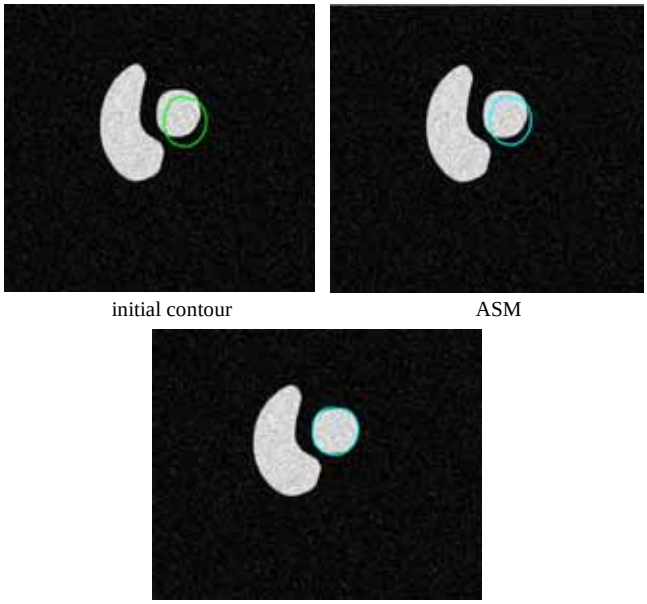

Fig. (5). Comparison of segmentation results, between the conventional ASM and the proposed method, on noisy synthetic images.

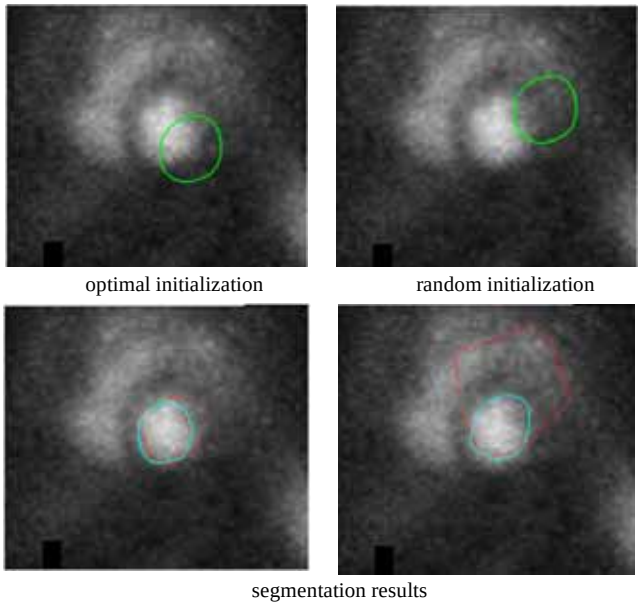

Fig. (6). Comparison of segmentation results, with various initializations, between the conventional ASM (in red) and the proposed method (in blue) on real scintigraphic images.

3. EXPERIMENTAL RESULTS

To evaluate the performance of the proposed segmentation method, we begin by applying it for the localization of a single object before presenting a generalization of the process for multiple object localization. Tests were performed on synthetic images as well as on complex real-world scintigraphic and MRI images.

3.1. Single object localization

In order to demonstrate its accuracy and its robustness, the proposed segmentation method has been used for the delineation of a single region of interest in synthetic images as well as in real-world medical images. On one hand, we have built a dataset composed of *18* noisy synthetic images, of size *550×400* pixels. Eight images were used for the training phase and the remaining ten images for the test phase. These images show clearly the contours objects, and then enable us to evaluate the behavior of the segmentation method against several challenges (sensitivity to initialization, presence of noise…). We compare the results of the proposed method with those produced by the conventional ASM, for the localization of a single object in noisy images with different initializations. In fact, we tested two configurations (Fig. (**5**)): optimal initial contour (close to the target object) and random initial contour (far from the target object). The obtained results confirm the inaccuracy of the conventional ASM, since good results are recorded only when the initial contours are close to the ROI. However, the introduction of the direction constraint has attenuated remarkably this limit, what proves that the proposed model allows more robustness against the initialization step, comparatively to the conventional ASM. Also, it is clear that the noise does not significantly affect the localization results especially in the first case when the initialization is optimized (close to ROI). Indeed, we distinguish the divergence of the standard ASM model while the proposed model has converged to the ROI despite the presence of noise and that the initialization was random (far from ROI). This proves the robustness of the proposed model against the noise and the initialization step. In fact, the integration of the spatial relationship allows an accurate extracting of the object of interest, even if the initialization is relatively remote and the noise is intensively present.

On the other hand, we used the proposed method for detecting the left ventricle of the heart, given a set of scintigraphic images showing the different possible shapes of heart during its beating cycle. These images have low contrast, low resolution, and the objects contours are hard to extract. This is why the objects localization is difficult in such images. We used a variety of images that come from *10* different patients. Indeed, the used dataset contains *10* sequences of scintigraphic images of the heart. From each sequence, composed of *16* images of size *128×128* pixels, we chose some images for the training phase to cover the different variations and we used the remaining images for testing the segmentation performance. Our goal is to detect the left ventricle of the heart in these ill-contrasted images. To do this, we compared the segmentation results before and after the integration of the spatial constraint (Fig. (**6**)), for various initializations (optimal *vs.* random). We can clearly conclude that, comparatively to the conventional ASM, the proposed method is much less sensitive to the initialization, what confirms its reliability for ROI detection. In fact, according to the realized tests, we can confirm that the shape constraint of the conventional ASM is unable alone to avoid that the contour is conducted towards other regions of the same visual appearance. However, the integration of the constraint direction into the ASM model, improves significantly the results of the segmentation, since this constraint limits the movement of the contours thereabouts real edges of the ROI.

Moreover, in order to evaluate visually the recorded results, we performed a comparison of the ASM with and without the introduced spatial constraint with respect to ex-

pert contour (given a ground-truth). We attempted to confirm this visual rendering through the comparison of obtained localization with the expert delineation. This comparison shows that the suggested method is particularly close to the expert segmentation (Fig. (**7**)). Indeed, the fuzzy directional constraint attracts the initial contour to the ROI, since the trace of the evolution of the initial contour's deformation is oriented directly to the target object. Unlike the conventional ASM, the deformation of the contour moves towards the similar appearance objects, while largely avoiding the contour displacement towards another object having the same visual appearance. Thus, the segmentation using the ASM integrating the spatial constraint is more accurate than the ASM without this constraint. We have also evaluated objectively the produced results, while measuring the distance between the ground-truth contours (manually defined by an expert) and the ones detected by the proposed model and by the conventional ASM, respectively. In fact, we used a modified version of the Hausdorff distance (*MHD*) [17] to assess quantitatively the degree of similarity (7) between the contour of the expert (*EC*) and the outline segmentation result (*CR*), for a set of 11 challenging images. In order to compare the results of both techniques, we chose two different scenarios: an optimal initialization of the contour and a random initialization of the contour. We remark that the recorded *MHD* values by the proposed model are lower than the values coming from the classic ASM (Fig. (**8**)). This proves that the proposed method is much more accurate, independently of the choice of the initial contour. In fact, in the case of an optimal initialization (resp. random initialization) the mean MHD distance is 3.19 (*resp.* 19.46) for the standard ASM and only 2.19 (*resp.* 2.43) for the proposed model. These results confirm the reliability and the robustness of the proposed model compared to the conventional ASM. Indeed, segmentation after integrating the spatial constraint is similar to the segmentation of the expert regardless of the position of the initial contour, even in the presence of noise, low resolution, low contrast and the presence of nearby objects with similar intensities.

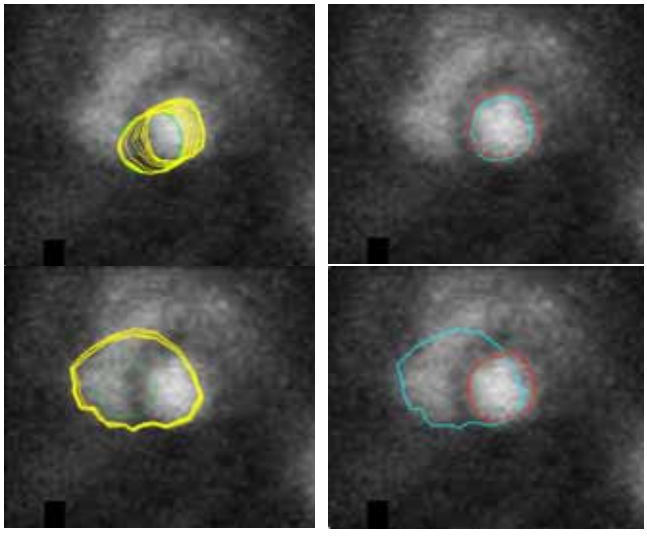

Fig. (7). Comparison of the evolution of the deformations (in yellow) of the initial contour (in green) between the proposed method (first row) and the conventional ASM (second row), with respect to expert contour (in red), on real scintigraphic images (final contour in blue).

$$MHD(\mathrm{CE},\mathrm{CR}) = \frac{1}{\aleph}\sum_{p\in CE} d(\mathrm{p},\mathrm{CR}), \tag{7}$$

where, $\aleph$ is the number of pixels of the expert contour *CE* and *d(p,CR)* denotes the distance between a pixel *p* of the expert contour *CE* and the nearest pixel in the detected contour *CR* (8).

$$d(\mathrm{p},\mathrm{CR}) = \min_{p'\in CR}\|p-p'\|. \tag{8}$$

3.2. Multiple Object Detection

The suggested segmentation method has been also used for the delineation of many objects of interest in noisy synthetic images as well as in real-world medical images. On one hand, we have built a dataset containing *18* noisy synthetic images of size *550×400* pixels. Eight images were used for the training phase and the remaining ten images for the test phase. As previously described, synthetic images were used to evaluate the performance of the proposed method in ideal cases because of having a very well contour description. Of course, we will not repeat the same tests already done with images containing a single object, since the dependence of results against the initialization and/or the presence of noise is not related to the number of objects to be detected. However, it is related to the proposed deformation process. We note that the results of object detection are encouraging for the case of synthetic images. Indeed, the proposed segmentation method was able to delineate precisely the set of objects of interest. In addition, the final contour (Fig. (**9**)) is almost close to the expert contour (in red). This permits an accurate localization of the ROI and affirms the reliability of the proposed segmentation method in the case of multiple objects even in the presence of noise.

On the other hand, we applied the proposed method on real-world MRI images which are collected from the Web [18]. These cerebral images, which contain multiple objects (caudate nucleus, thalamus, putamen…), are challenging since they are characterized by the absence of visible contours between structures of interest and by the anatomic variability of these structures. The used dataset contains MRI brain sections and each image is composed of *255×255* pixels. We chose some images to cover the various changes during the training step, while representing the widest possible set of studied shapes. In Fig. (**10**), we show the results of the detection of the caudate nucleus and the putamen in a cerebral MRI image. We note that the localization results are very precise, and the proposed model converges to the desired ROI even under low contrast and low resolution constraints. In fact, final contours are almost close to the expert contours (in dashed). As we have seen, the integration of the direction constraint into ASM allows the segmentation of many objects with worse contours definition in low-resolution and low contrast images. Indeed, the integration of the direction constraint forced the shape model to move in an acceptable space of orientations, what avoids collisions and remoteness of the shape model. This demonstrates the effectiveness of the proposed method even in the presence of neighboring structures of similar intensities. In fact, the integrated spatial constraint permits the reduction of the ASM sensibility against the initialization and the presence of noise.

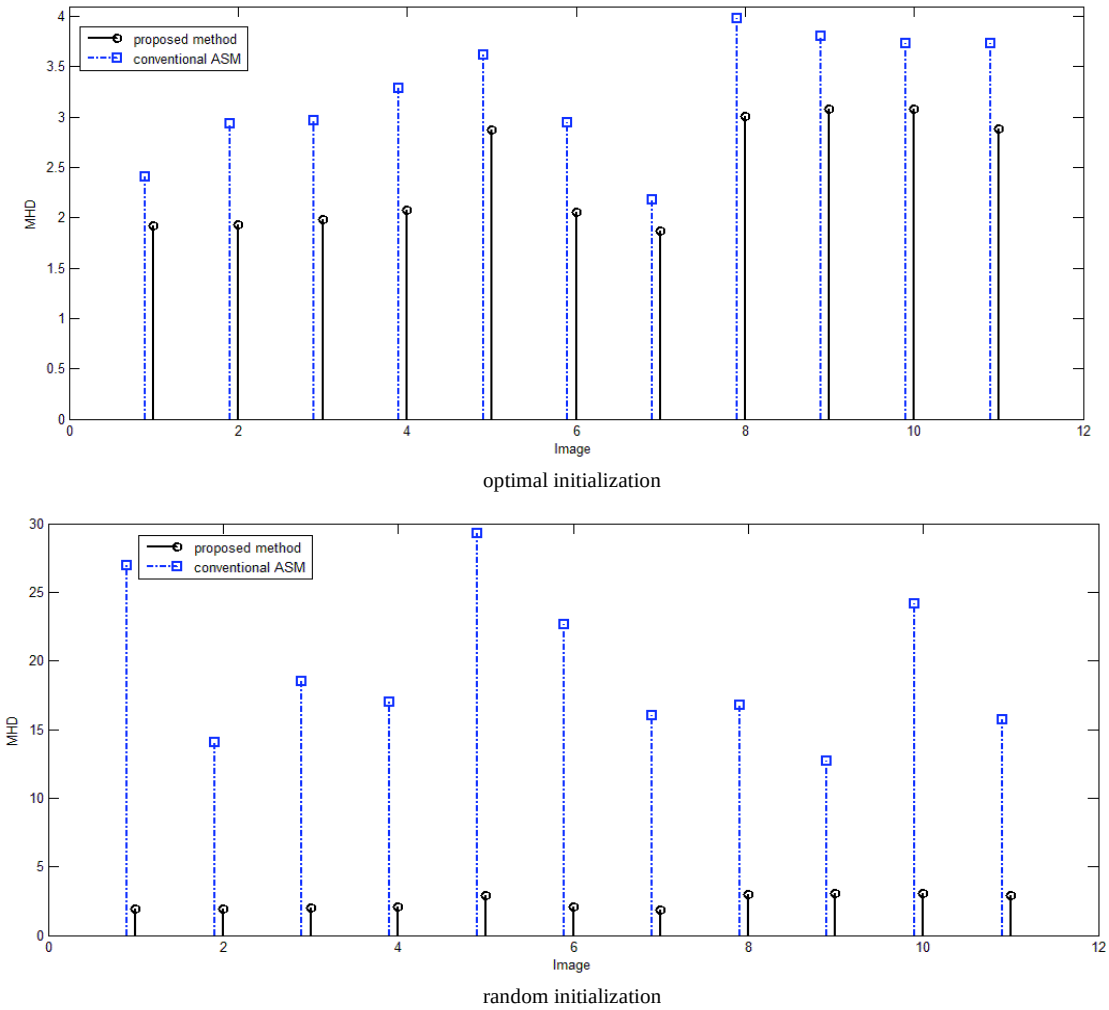

Fig. (8). Comparison of the *MHD* distance between the proposed method and the classic ASM.

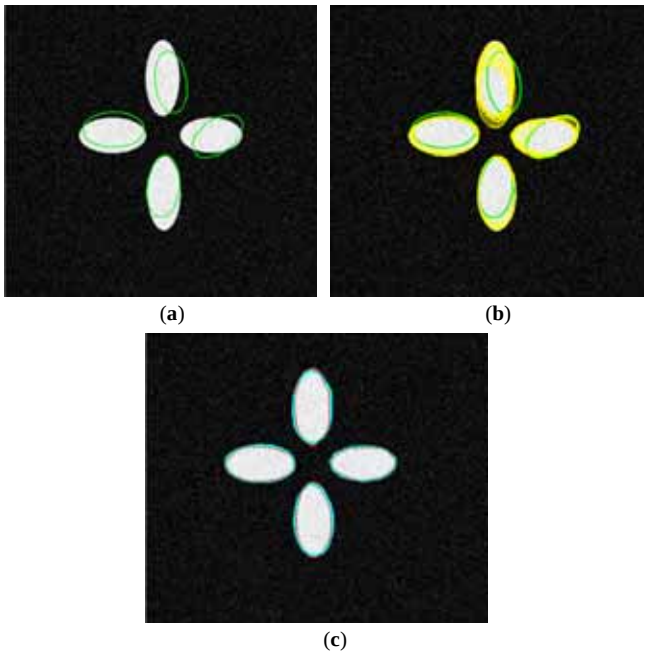

Fig. (9). Multiple object detection in a noisy synthetic image: (**a**) initial contours, (**b**) evolution of the deformations, (**c**) final localization of ROI.

4. CONCLUSION AND FUTURE WORKS

A reliable method for medical image segmentation with prior knowledge is proposed in this paper. This method is based on the integration of a fuzzy spatial relationship constraint of direction into the active shape models. Thus, an angle model is combined with the shape angle of ASM in order to advantageously exploit the maximum of a priori knowledge for an accurate delineation of the studied objects, since these objects are anatomical and functional structures associated to medical knowledge. Extensive experiments were performed on synthetic noisy images as well as on real-world MRI and scintigraphic medical images with low contrast and low resolution. The recorded results on the tested images, for which difficulties arise because of the complexity of the target objects, showed the robustness of the proposed method for accurate tracking and detection of ROI, even in noisy and ill-contrasted images. In addition, in comparison with the conventional ASM, results show that the proposed model converges to the desired ROI even in the presence of noise and regardless of the position of the initial contour. Thus, the spatial relationship is a key of both robustness and accuracy, and the obtained results, whether on synthetic or on real-world images, show the contribution of the integration of the direction constraint. Indeed, adding the

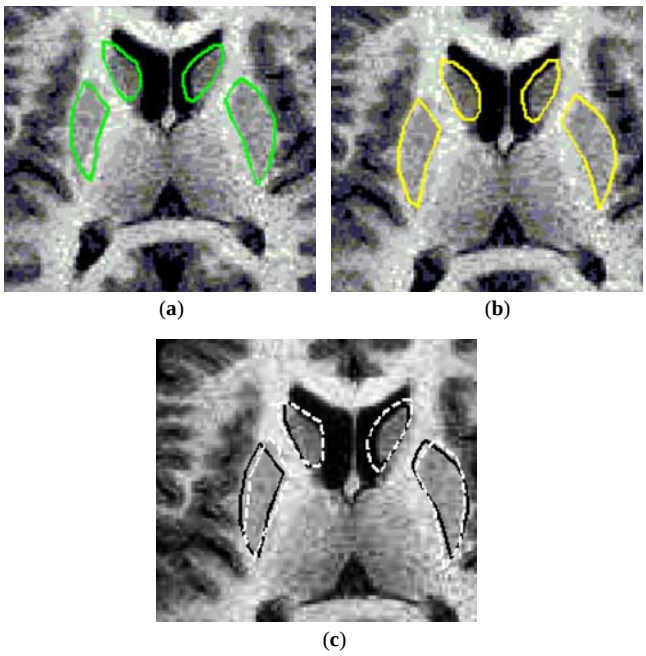

(**a**) (**b**)

(**c**)

Fig. (10). Multiple object detection in a magnetic resonance image of the brain: (**a**) initial contours, (**b**) evolution of the deformations, (**c**) final localization of ROI.

angle constraint to ASM improves remarkably the segmentation accuracy as this constraint limits the contours' movement towards other objects. However, the allowable space of angles' variation can be very huge, particularly if we used a large training set, what limits the contribution of the proposed method. To alleviate this limitation, we propose to incorporate additional prior knowledge about spatial relationships to improve the quality of segmentation. Among spatial relationships that can be efficiently incorporated into the ASM, we can mention the distance separating two or many objects in the same image, and notably the symmetry that characterizes most of the medical images. We also plan to extend the proposed method for the general case of medical image sequences.

CONFLICT OF INTEREST

The authors confirm that this article content has no conflict of interest.

ACKNOWLEDGEMENTS

Declared none.

REFERENCES

[1] Ahmad E, Yap MH, Degens H, McPhee JS. Atlas-registration based image segmentation of MRI human thigh muscles in 3D space. Proceedings of SPIE 9037, Medical Imaging 2014: Image Perception, Observer Performance, and Technology Assessment; 2014 Mar 11; San Diego, USA.

[2] Tsechpenakis G. Deformable model-based medical image segmentation. In: El-Baz AS, Acharya RU, Mirmehdi M, Suri JS, Eds. Multi modality state-of-the-art medical image segmentation and registration methodologies. New York: Springer 2011; pp. 33-67.

[3] Rueckert D, Schnabel JA. Registration and segmentation in medical imaging. In: Cipolla R, Battiato S, Farinella GM, Eds. Registration and recognition in images and videos. Berlin: Springer 2014; pp. 137-56.

[4] Kass M, Witkin A, Terzopoulos D. Snakes: Active contour models. Int J Comput Vision 1988; 1(4): 321-31.

[5] Osher S, Sethian JA. Snakes: Fronts propagating with curvature dependent speed: Algorithms based on Hamilton-Jacobi formulations. J Comput Phys 1988; 97(1): 12-49.

[6] Cootes TF, Taylor CJ, Cooper DH, Graham J. Snakes: Active shape models - Their training and application. Comput Vis Image Und 1995; 61(1): 38-59.

[7] Jaafar B, Khlifa N. A Conception of a 2D active-shape model integrating a spatial relation card based on a fuzzy logic. Proceedings of International Conference on Communications, Computing and Control Applications; 2011 Mar 3-5; Hammamet, Tunisia.

[8] Ghose S, Mitra J, Oliver A, *et al*. A supervised learning framework for automatic prostate segmentation in trans rectal ultrasound images. Proceedings of International Conference on Advanced Concepts for Intelligent Vision Systems; 2012 Sep 4-7; Brno, Czech Republic.

[9] Fouquier G, Atif J, Bloch I. Snakes: Sequential model-based segmentation and recognition of image structures driven by visual features and spatial relations. Comput Vis Image Und 2012;116(1): 146-65.

[10] Ettaieb S, Khlifa N, Hamrouni K. ASM+D: Nouveau modèle de formes actives intégrant une relation spatiale de distance. Proceedings of GRETSI; 2009 Sep 8-11; Dijon, France.

[11] O'Brien S, Ghita O, Whelan PF. Segmenting the left ventricle in 3D using a coupled ASM and a learned non-rigid spatial model. Proceedings of International Conference on Medical Image Computing and Computer Assisted Intervention; 2009 Sep 20-24, London, UK.

[12] Xinjian C. Snakes: 3D automatic anatomy segmentation based on iterative graph-cut-ASM. Med Phys 2011; 38(8): 4610-22.

[13] Zheng Q, Lu Z, Feng Q, *et al*. Adaptive segmentation of vertebral bodies from sagittal MR images based on local spatial information and Gaussian weighted chi-square distance. J Digit Imaging 2013; 26(3): 578-93.

[14] Chen X, Udupa JK, Alavi A, Torigian DA. GC-ASM: Synergistic integration of graph-cut and active shape model strategies for medical image segmentation. Comput Vis Image Und 2013; 117(5): 513-24.

[15] McIntosh C, Burnaby BC, Hamarneh G. Medial-based deformable models in nonconvex shape-spaces for medical image segmentation. IEEE T Med Imaging Und 2013; 31(1): 33-50.

[16] Bilgin G. Evaluation of spatial relations in the segmentation of histopathological images. Proceedings of Signal Processing and Communications Applications Conference; 2013 Apr 24-26, Mersin, Turkey.

[17] Barhoumi W, Zagrouba E. Boundaries detection based on polygonal approximation by genetic algorithms. In: Damiani E, Howlett RJ, Jain LC, Ichalkaranje N, Eds. Frontiers in Artificial Intelligence and Applications. New York: Springer 2002; pp. 1529-33.

[18] Menze B, Jakab Z, Bauer S, Reyes M, Prastawa M, Leemput KV. MICCAI 2012 challenge on multimodal brain tumor segmentation. 2012. Available from: www2.imm.dtu.dk/projects/BRATS2012 [cited: 19th Jan 2014]

Received: August 18, 2014 Revised: January 25, 2015 Accepted: March 03, 2015